

Article

# Monitoring Cultural Heritage Sites with Advanced Multi-Temporal InSAR Technique: The Case Study of the Summer Palace

Panpan Tang <sup>1,2</sup>, Fulong Chen <sup>1,2,\*</sup>, Xiaokun Zhu <sup>3</sup> and Wei Zhou <sup>1,2</sup>

<sup>1</sup> Key Laboratory of Digital Earth Science, Institute of Remote Sensing and Digital Earth, Chinese Academy of Sciences, No. 9 Dengzhuang South Road, Haidian District, Beijing 100094, China; tangpp@radi.ac.cn (P.T.); zhouwei@radi.ac.cn (W.Z)

<sup>2</sup> International Centre on Space Technologies for Natural and Cultural Heritage under the Auspices of UNESCO, No. 9 Dengzhuang South Road, Haidian District, Beijing 100094, China

<sup>3</sup> Beijing Institute of Surveying and Mapping, No.15 Yangfangdian Road, Haidian District, Beijing 100038, China; zhuxk@radi.ac.cn

\* Correspondence: chenfl@radi.ac.cn; Tel.: +86-10-8217-8198; Fax: +86-10-8217-8915

Academic Editors: Rosa Lasaponara, Zhong Lu and Prasad S. Thenkabail

Received: 12 March 2016; Accepted: 17 May 2016; Published: 21 May 2016

**Abstract:** Cultural heritage sites are rare and irreplaceable wealth of human civilization. The majority of them are becoming unstable due to a combination of human and natural disturbances. High-precision, efficient deformation monitoring facilitates the early recognition of potential risks and enables preventive diagnosis of heritage sites. In this study, an advanced Multi-Temporal Interferometric Synthetic Aperture Radar (MTInSAR) approach was developed by jointly analyzing Persistent Scatterers (PSs) and Distributed Scatterers (DSs) using high-resolution SAR images. Taking the World Heritage Site of Summer Palace in Beijing as the experimental site, deformation resulting from PSs/DSs showed that overall the site was generally stable except for specific areas and/or monuments. Urbanization (construction and demolition) triggered new subsidence in the vicinity of East and South Gate of the site. Slight to moderate (mm/cm-level) instabilities of ruins and monuments on Longevity Hill were detected, perhaps due to a combination of destructive anthropogenic activities and long-term natural decay. Subsidence was also detected along the Kunming Lakeside and was probably attributable to variation of the groundwater level, excessive visitor numbers as well as lack of maintenance. This study presents the potential of the MTInSAR approach for the monitoring and conservation of cultural heritage sites.

**Keywords:** cultural heritage sites; instabilities; MTInSAR; Distributed Scatterers; the Summer Palace

## 1. Introduction

As the legacy of physical artifacts and intangible attributes of a society, cultural heritage is inherited from past generations and serves in the understanding of cultural diversity as well as the evolutionary relationship between earth and humans. Considering educational and inspirational functions, cultural heritage contributes to world peace and security [1]. Cultural heritage sites, referring to the locations of historical structures and monuments such as ancient palaces, churches, tombs and bridges, are rare, irreversible and irreplaceable wealth of humanity [2]. Unfortunately, they are often impacted by natural calamities and anthropogenic activities. The former includes landslides, earthquakes, floods, adverse weather and abrupt climate change. However, more serious and increasing threats could originate from wars, overexploitation, urbanization and uncontrolled tourism. Consequently, monitoring and preventive diagnosis are essential for the safeguarding and conservation of cultural heritage sites.

Generally, structural and ground instabilities can be jointly triggered by the subtle, long-term movements at the mm-level due to natural erosions, ground displacements or crust movements. Abrupt deformations due to drastic events such as earthquakes, landslides and impacts of war may cause more significant, *i.e.*, at least cm-level, shifts [3]. According to [4,5], historic structures are subjected to potential elastic deformation and brittle collapses are extremely common in cultural heritage sites. Monitoring the deformation of structures as well as their surroundings facilitates the early recognition of potential risks and enables effective conservation planning. Traditional investigations, including leveling, GPS surveying and geophysical prospecting are restricted by their limited spatial/temporal coverage as well as the need for considerable human and financial resources. Furthermore, some of the traditional approaches are invasive, such as installing electrical sensors in structures for data acquisition [3]. Multi-Temporal Interferometric Synthetic Aperture Radar (MTInSAR) techniques (e.g., Persistent Scatterers (PSInSAR) [6], Small Baseline Subsets (SBAS) [7], and SqueeSAR [8]), rely on processing of multi-temporal repeat-pass SAR images to measure phase signals of radar targets. They overcome the shortcomings of traditional methods referred to above and provide a framework for large-scale and high-precision (from cm to mm level) deformation monitoring. The results of MTInSAR also facilitate the understanding of motion patterns in the spatial domain by clarifying the ongoing deterioration phenomena related to natural/human processes [9]. Consequently, MTInSAR techniques are often recommended as an effective tool to monitor cultural heritage sites at scales ranging from single monuments to heritage site covering large areas [3,9–14].

This study focuses on the assessment of cultural heritage sites exposed to subtle movements due to environmental and human-induced factors, in the range from millimeters to centimeters. Compared with devastating, abrupt displacements, subtle motion is more common and imperceptible in heritage sites, particularly considering its long-term, pernicious impacts. Impacts of urbanization processes, where demolitions or construction activities as well as the exploitation of groundwater and natural resources are intense, could be magnified by erosion from extreme weather and together synergistically trigger deformations of surface and/or artifacts. Though MTInSAR techniques have been effective in allowing a quantitative estimation of subtle displacements, current approaches [6–8] have limitations due to the small amount of SAR images available or to the sparse spatial density of measurable points. To solve those problems, an advanced methodology, jointly analyzing Persistent Scatterers (PSs) and Distributed Scatterers (DSs), characterized by small spatial/temporal baselines [15,16], was developed. PSs refer to objects that maintain strong and stable backscattering over a long period; historic monuments are good examples of PSs. DSs correspond to homogeneous surfaces with similar backscattering characteristics in the SAR images, including ruins, bare ground or meadows. The occurrence ratio of PSs to DSs differs significantly in environments populated by heritage sites due to the difference of structural types and vegetation covers. The enhancement of measuring points could have a significant and positive impact on the monitoring results by integrating PSs and DSs. Furthermore, the use of the small-baseline strategy relaxes the requirement of SAR data in conjunction with the mitigation of phase noise induced by the spatial-temporal decorrelation.

High-resolution SAR images, e.g., TerraSAR/TanDEM-X, COSMO-SkyMed, Radarsat-2 and ALOS PALSAR-2, are recommended for risk monitoring of local-scale monuments [3]. In this paper, first the description of the study site and data used are provided. Then the processing methodology for SAR data and the proposed advanced MTInSAR methodology are introduced. This is followed by data analyses and discussion of deformation results and instability mechanisms. Afterwards, the methodology used is validated using groundwater data and the observed phenomena from field investigations. Finally, important conclusions are drawn.

## 2. Study Area

Due to its long and rich (over 5000 years) civilization, China is well-known for the amount and diversity of its cultural heritage sites (33 of them have been listed in the UNESCO World Heritage List up to 2015). However, the sustainability of China's heritage sites is facing challenges due to frequent

natural hazards such as earthquakes and landslides. Rapid socio-economic development, which often results in overexploitation of sources of ground water and/or energy, urbanization and uncontrolled tourism, are also posing growing threats to these sites. In this study, the feasibility and capability of satellite MT-InSAR technology for cultural heritage risk monitoring and preventive diagnosis have been investigated by taking the Summer Palace (in the northwest of Beijing City) as the experimental site. The geological condition in the Beijing City is uniform, which is predominated by the plain loose deposits, including soils that are sandy loam, sand and gravel, with a thickness of dozens of meters.

Formerly known as the “Qingyi Garden”, Summer Palace was an imperial garden during Ming and Qing dynasties; it has been a World Cultural Heritage site since 1998 and is also one of the most heavily visited attractions in China. The palace stretches about 2.97 square kilometers comprising Kunming Lake (covering three quarters of the total area of the site), Longevity Hill and other features for imperial affairs or recreation (see Figure 1). Kunming Lake, with a maximum depth of over 3 m, was once a natural lake but was later artificially modified to provide water supply for the residents of the Palace. Three islands are located on the lake surface. Longevity Hill, located at the north shore of the lake, rises to a maximum elevation of 108 m. It is made of rocks (mainly sandstone and shale) and cinnamon soils as evidenced by samples collected from the bottom of the Kunming Lake. Longevity Hill was first named by Emperor Qianlong in 1751 (AD).

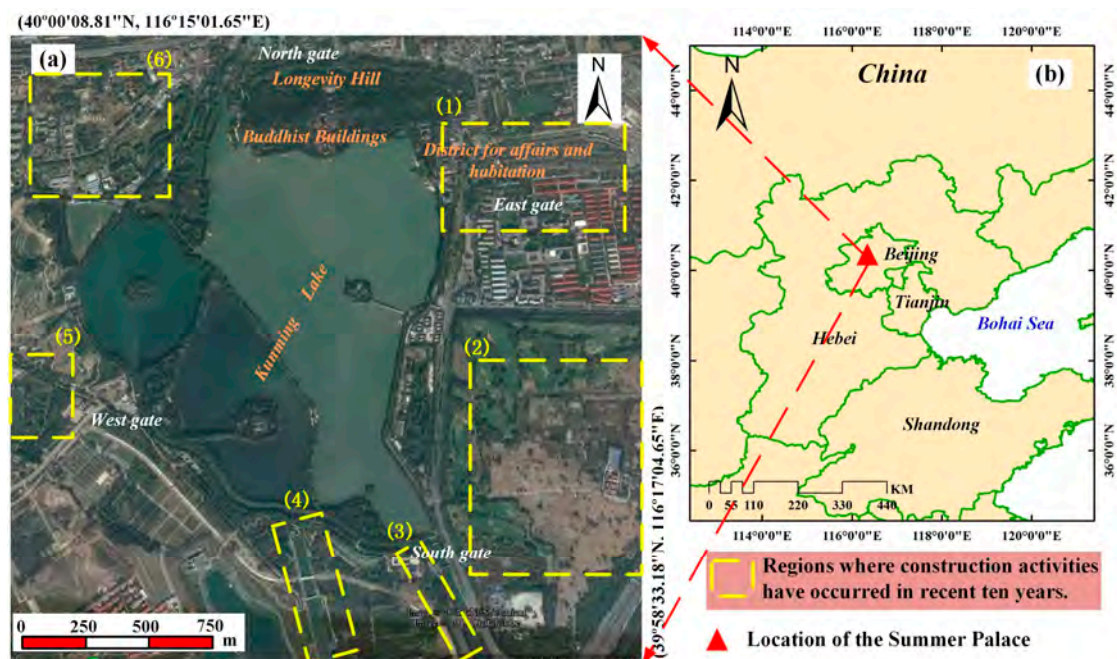


**Figure 1.** (a) Summer Palace study area (courtesy of Google Earth) with construction zones indicated by yellow dashed lines; and (b) location of the Summer Palace.

Most buildings in the Summer Palace were burned down by Anglo-French forces in 1860, and then in the next 150 years, some of them were rebuilt and renovated many times while others were left as ruins. Nowadays, more than 3000 historic buildings remain in the site for Buddhist incense, government affairs, imperial rest and recreation. As Chinese traditional architecture, patterns include pavilions, towers, archways, halls, long corridors and bridges. The majority of them are made of glazed tiles, wood and stone foundations.

The landscape surrounding Summer Palace has experienced enormous changes, including the construction of roads, subways, buildings, parks and an artificial riverway, as well as the demolition of dilapidated residential structures. Behaviors in six typical regions, marked by yellow boxes in Figure 1a, are described in detail (Table 1). Construction activities in Region 1, in the vicinity of historic structure-complex, lasted seven years. The ground disturbance from heavy vehicles and digging

activities induced instabilities of adjacent buildings. In Region 4, the implementation of a “Water Diversion Project” changed the water level of Kunming Lake temporarily and has probably affected the hydrological condition of islands, boatyards and other historic buildings surrounding the Lake. In contrast, impacts of Regions 2, 3, 5 and 6 on monuments were probably negligible since they are further away from the principal monuments.

**Table 1.** Descriptions of construction and demolition activities in the vicinity of the heritage site.

Region	Location (of the Site)	Events	Duration	Potential Impacts
(1)	East gate	Construction of a residential area and a subway station	2003~2010	Causing instabilities of historic buildings near the East gate
(2)	Southeast	Demolition of Liulang Village	2010~2013	Causing instabilities of roads and buildings around the site
(3)	South gate	Construction of a highway	April 2006~2009	Negligible
(4)	South	Construction of a riverway as part of a “Water Diversion Project”	May 2006~2009	Water level of Kunming Lake reduced
(5)	West gate	Demolition of a residential area and creation of a garden	2010~2012	Negligible
(6)	Northwest	Redevelopment of a shanty town	2005~2011	Negligible

### 3. Data

In this study, the changes of the heritage site, particularly the motion anomalies, were assessed by radar interferometry. Twenty scenes of x-band (radar frequency of 9.6 GHz) COSMO-SkyMed SLC images were used for the analysis. They were acquired along descending orbits with the “Stripmap Himage” and “HH polarization” mode, spanning from January 2009 to October 2010. The center incidence angle was approximately  $20.2^\circ$  and the pixel spacing is 0.769 m and 2.266 m in range and azimuth direction, respectively. Precipitation for 2009–2010 and groundwater data for 2008–2010 were collected from Beijing Water Authority. During those two years, Beijing experienced a period of drought with the annual precipitation ranging between 480 and 524 mm, well below long-term average value of 558 mm over the last 30 years (see Figure 2a). Furthermore, approximately 80% of the rainfall during 2009–2010 occurred in the summer, from June to September. Figure 2b illustrates the changes in groundwater level (averaged values from boreholes in downtown locations) of Beijing City during the period of 2008–2010. A declining trend can be observed with an average value of approximately 2.7 m. As a man-managed reservoir, Kunming Lake generally stores water in spring for the tourism and draws off a certain volume for security purposes before the freezing season, resulting in the water-level rises in summer and falls-off in winter. In the observation period of 2009–2010, the lake level descended more than half a meter during summer (reported by administrators), coinciding with the decline trend of the groundwater level (see Figure 2b).

One arc-second (spatial posting of 30 m) Shuttle Radar Topography Mission (SRTM) Digital Elevation Model (DEM) was obtained from the United States Geological Survey (USGS, <http://earthexplorer.usgs.gov/>) for the topographic phase removal and InSAR-derived products geocoding. Google Earth images (© 2013 Google Inc., Mountain View, CA, USA) were used for the illustration and interpretation of geocoded InSAR results.

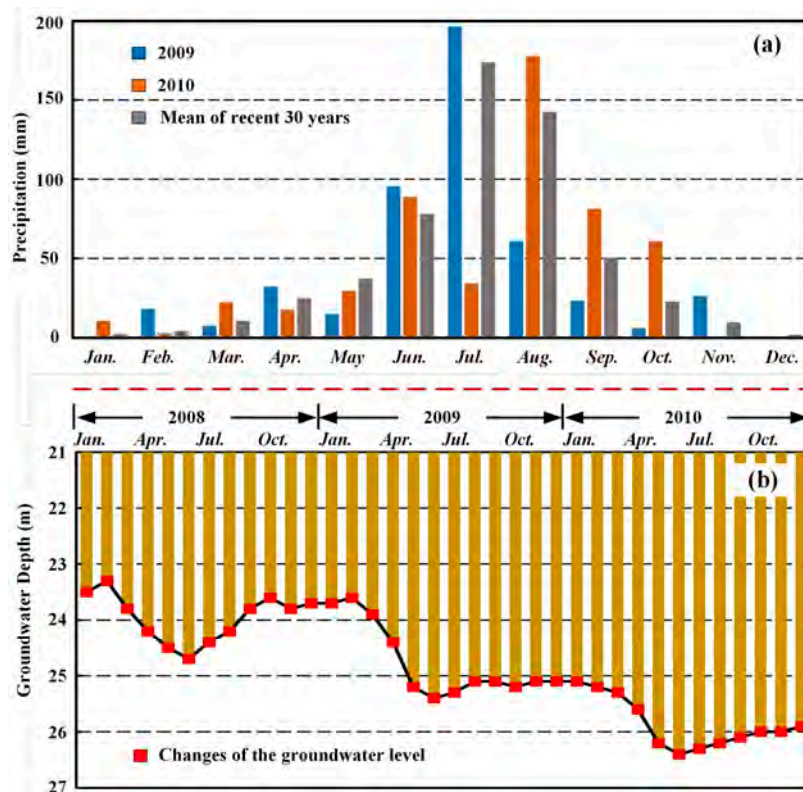


**Figure 2.** (a) Monthly precipitations of 2009 and 2010 and the mean values calculated from the last 30 years; and (b) groundwater variations of Beijing City in the period of 2008–2010.

#### 4. Methodology and Experimental Procedures

Monitoring the deformation of cultural heritage sites by advanced MTInSAR approach proposed herein is a complex task. The entire data processing and interpretation flow is shown in Figure 3. A comprehensive background investigation is recommended as a first step to obtain detailed data and knowledge of the characteristics of the site with regard to landscape, ground features, spatial scale, and geometric and material properties [3]. These measures facilitate the choice of hot spots, the adoption of efficient data processing techniques [11] and the identification of monuments. In general, there is a close link between regional surface displacements and the monument structural instabilities. As for the Summer Palace, historic architectures, ruins, slopes of Longevity Hill and the surrounding surface were systematically monitored.

An efficient SAR data processing procedure was developed and executed after preliminary investigation. In this study, calibrated single-look complex (SLC) images were firstly co-registered referring to the master image (20091120), resulting in high accuracy with a standard deviation limited to 0.02 pixels. Then, massive historic architectures in the Summer Palace were extracted as PS candidates using the indexes of strong backscattering and low intensity-variability [17]. The spatial distribution of PSs was usually uneven due to the diversity of observed features. The scarcity of PS points could hamper the estimation of atmospheric delay and deformation parameters [16]. Therefore, DS points were further introduced to enhance point density. A Kolmogorov–Smirnov test was applied to identify homogeneous pixels using the amplitude of multi-temporal SAR images. Pixels with more than 180 homogeneous neighbors in a sliding  $20 \times 20$  (pixels) window were extracted as DS candidates. The merging of the distributions of PSs and DSs is illustrated in Figure 4a, covering the whole study area except for the Lake surface and densely vegetated regions. Due to the high resolution of SAR images, ancient buildings and ruins located on the Longevity Hill (planted with more than 1600 old trees) were detected even in locations that were partly covered by trees. Generally, the

performance of traditional MTInSAR approaches (e.g., extracting only PSs [18] or Coherent Scatterers (CSs)) could be rather limiting, because the majority of ruins or bare ground among trees belong to DSs based on the backscattering. Moreover, the coherence estimation of CSs could be affected by vegetation. Compared with PSs, DSs usually maintain a low signal-to-noise-ratio (SNR) and a de-noised coherence. The approach of phase optimization in SqueeSAR™ [8] and the LBFGS (Limited memory Broyden–Fletcher–Goldfarb–Shannon) algorithm were adopted for the phase reconstruction of DS points after the procedure of an adaptive homogenous filtering [19–21]. The algorithm of LBFGS has similar performance in resolving nonlinear problems compared with quasi-Newton methods [22].

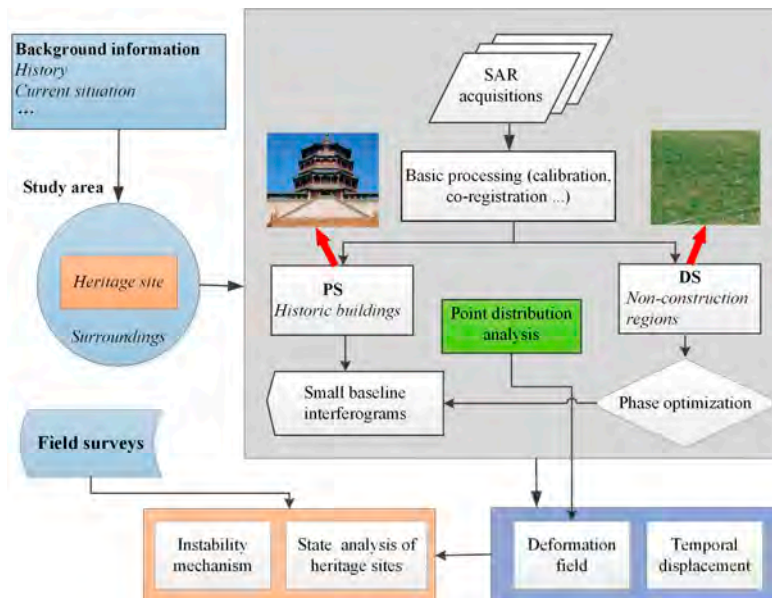


**Figure 3.** Flow chart of the data processing and interpretation for the monitoring of heritage sites using the advanced Multi-Temporal Interferometric Synthetic Aperture Radar (MTInSAR) approach.

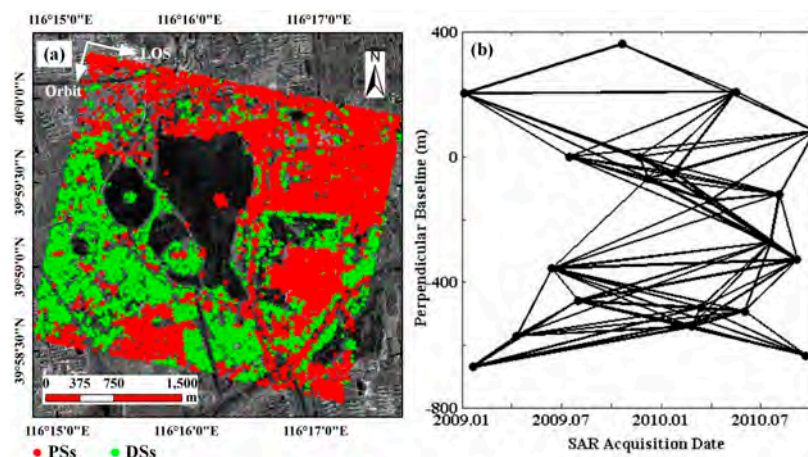


**Figure 4.** (a) Distribution of Persistent Scatterers (PSs) and Distributed Scatterers (DSs) in the Summer Palace and its surroundings; and (b) interferograms with spatial and temporal baselines (circles indicate SAR acquisitions).

Based on the candidate points, the procedure of SBAS technique was applied to estimate the unknown parameters (e.g., deformation rates and residual heights) in order to mitigate the constraint of SAR image numbers as well as to enhance the interferogram coherence. Eighty-three differential interferograms with small orbital and temporal baselines (see Figure 4b) were derived after removing

the topography and earth flat phases. 3D unwrapping algorithm (temporal and spatial domains) was applied to estimate the integer ambiguities of the wrapped phase [23]. Topography errors and deformation rates were derived by the least squares solution, and then the atmospheric delay and non-linear displacements were separated by applying temporal/spatial filters. Displacements in this study were in the line of sight (LOS) direction (center incidence angle of  $20.2^\circ$ ); minus values indicated targets moving away from satellite (subsidence) and *vice versa* (uplift). Note that InSAR techniques measure relative rather than absolute deformation values. A precision, better than 1.0 mm/a, can be derived on neighborhood points. In this study, regions with motion values from  $-1$  to  $+1$  mm/a were assumed to be stable.

By integration of the merits of SBAS and SqueeSAR, an advanced MTInSAR methodology was developed to monitor heritage sites experiencing mm-level movements. A large number of measurable points (PSs and DSs) were extracted on the site with a semi-natural landscape. The minimized phase noise from the spatial-temporal decorrelation in conjunction with the relaxed data requirement of PSInSAR and/or SqueeSAR techniques can be achieved by utilizing the small-baseline strategy. Basic interferometric processing (including SLC SAR image calibration, SAR image co-registration, multi-looking, PS candidate extraction, interferogram generation, removal of topography and flat earth phase and 3D phase unwrapping) was carried out using GAMMA software [17]. For other stages of the interferometric processing, programs implemented in MATLAB and C++ were applied (for more technical details, please refer to [16]).

## 5. Results and Validation

### 5.1. Results and Interpretation

According to the motion phenomena detected by the proposed MTInSAR technique, the whole palace was divided into the following four components for further interpretation and discussion: Longevity Hill, East Gate region, Kunming Lakeside and islands, and surrounding landscapes.

#### (1) Longevity Hill

The Longevity Hill can be divided into a southern and a northern part. In the southern part of the hill, there is a huge historic complex including the Pavilion of Buddhist Incense (a three-floored octahedral building). From the Lakeshore upward to the hill top, archway, gate of Dispelling Clouds, hall of Dispelling Clouds and Moral Glory, Pavilion of Buddhist Incense and Sea of Wisdom stand in proper sequence along the central axis. In the northern part, the Han-Tibetan style of Buddhist buildings and Suzhou Street are located. Besides the central axis, there are a few regions occupied by houses, monuments and ruins; however, they were unfortunately un-observable because of the lack of PS/DS points due to the dense vegetation. Figure 5a shows the distribution and annual deformation rates of PSs/DSs. PSs are easily identified corresponding to exposed targets such as the Pavilion of Buddhist Incense. It is difficult to identify DSs using optical images because of the cover and shadow effects of trees. Field investigations indicated that DSs extracted belong to ruins or barren areas among sparsely distributed trees.

Protective measures and/or consolidations have been periodically introduced, particularly for essential monuments; for example, iron sticks were installed to fasten wooden structures (a common countermeasure in the site). Deformation map (see Figure 5a) demonstrates that the entire Longevity Hill was relatively stable, with LOS rates ranging from  $-6.0$  to  $1.0$  mm/a. However, a few regional and individual instabilities were detected. Point A, with the deformation rate of  $-2.7$  mm/a, refers to the Hanxin pavilion located in the eastern hillside (see Figure 5b). The displacement evolution showed that the pavilion was stable until the end of 2009, and then subsided at a constant rate. Compared to the stable DSs measurements of the neighborhood, it implied that the instability was attributable solely to the structural degradation of the pavilion rather than its surrounding surface. Region 1 is located at the halfway down the hill, containing a pavilion named Chongcui (see Figure 5c) with a brick floor

that is favorable for the extraction of DSs. The deformation rate of  $-2.6$  mm/a reflected instabilities caused by the slope sliding in steep terrain. Point B belongs to a structure named Duiou (see Figure 5d), which used to be a waiting room but has now been converted into a boatyard and shop. Deformation results, with the deformation rate up to  $-3.2$  mm/a, indicated that it was unstable. Point C is in the region occupied by several shops and a boatyard (see Figure 5e), indicated a distinct subsidence with rates up to  $-4.5$  mm/a. Dense tourism flow, which would impose pressures on structures (e.g., overweight and destructive activities), combined with the water-level change explains the motion anomaly. Groundwater data were used to validate the evolution of Points B and C, indicating a consistent trend among the two observations. Another factor responsible for the instabilities could be the protracted maintenance or protection activities implemented in the area.

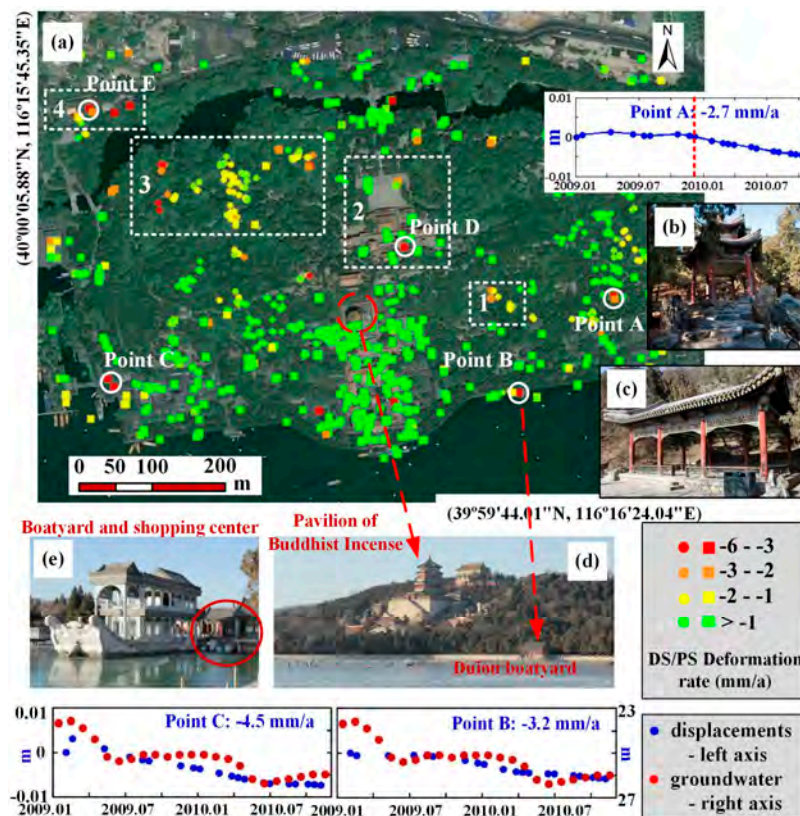


**Figure 5.** (a) Map of deformation rates of the Longevity Hill superimposed on the Google Earth image. Four typical regions (from Region 1 to Region 4) and five points (A–E) with significant motions are shown; (b–e) Photographs of Point A, Region 1, and Points B and C obtained during field campaigns, respectively. The three graphs illustrate displacement evolution (blue dots) of Points A–C; the red dashed line in the evolution of Point A was used to mark the starting time of subsidence. Groundwater data (red dots) were used to validate the motion evolutions of Points B and C.

At the north side of the Longevity Hill, three regions (Regions 2–4) were selected for analysis, and their corresponding photographs are illustrated in Figure 6. MTInSAR-derived results indicated that they were suffering from subsidence in the mm–cm level. Region 2 belongs to Sidabuzhou with several Buddhist buildings in the south and ruins in the north (see Figure 6a). Monuments here tended to be vulnerable over hundreds of years, validated by the surface damages or cracks on ancient walls. Point D indicated the instability of one historical building with a deformation rate of  $-6.7$  mm/a. Archaeological excavations were carried out in ruins since 2010 when SAR images started to be acquired, resulting in the extraction of sparse DSs. Several PSs with deformation rates over  $-2.0$  mm/a caused by the disturbance from human activities (e.g., archaeological excavations) were identified.



**Figure 6.** Photographs of Regions 2–4 marked in Figure 5a: (a) Region 2; (b) Region 3; and (c) Region 4. Displacement evolution of Points D and E (see Figure 5a for their locations) are illustrated by two sub-graphs.

Region 3 refers to three residual ruins covered by dense woods (see Figure 6b). Nobody would notice them if no DSs were extracted for those locations. The combined deterioration due to human activities and natural decay contributed to the instabilities in these Regions. For instance, nothing is left nowadays on Gaichun Yuan (used to be a beautiful garden located along the steep hillside) except for broken walls and residual pillars. DSs and PSs, with the maximum deformation rate of  $-3.9$  mm/a, were identified due to the strong signal echo from wall remains. The site in the middle (WeixianZhai) used to be a school palace of Emperor Qianlong. At present, only collapsed walls and residual pillars remain. Compared with the previous site, this region is more stable due to the flat terrain and deformation rate was  $-1.5$  mm/a on DS points. The west site refers to Qiwang Xuan, a garden connecting the Longevity Hill to the boatyard. As seen in the photograph, it is clear that the floor with a steep terrain was damaged due to subsidence with values up to  $-4.3$  mm/a. In Region 4, there are a group of houses named Tingli Guan (see Figure 6c), which used to be an imperial opera hall but today it is a famous restaurant. Instabilities of wood structures (e.g., cracks) could be observed on the walls and correspond to PSs with deformation rates up to  $-5.0$  mm/a (Point E).

## (2) East Gate Region

The historical artifacts near the East Gate were built for imperial affairs and habitation. The majority of them are well preserved, such as the Hall of Benevolence and Longevity where emperors used to deal with state affairs and receive foreign guests. The Hall of Joyful Longevity, with beautiful scenery, is the best place for habitation and entertainment considering its function for connecting the Longevity Hill and Kunming Lake. The Hall of Virtue and Harmony was previously famous as a theater. Wenchang Yard and Tower, which used to be an imperial kitchen and a sacrifice site, respectively, have been converted to a museum exhibiting cultural relics. Besides these historic monuments, plentiful of modern houses, entertainment and shopping centers, schools and a subway station, are located surrounding the heritage site. Urbanization has significantly changed the landscape of this region as shown by the growth of civilian constructions during 2009–2010 (see Figure 7a).

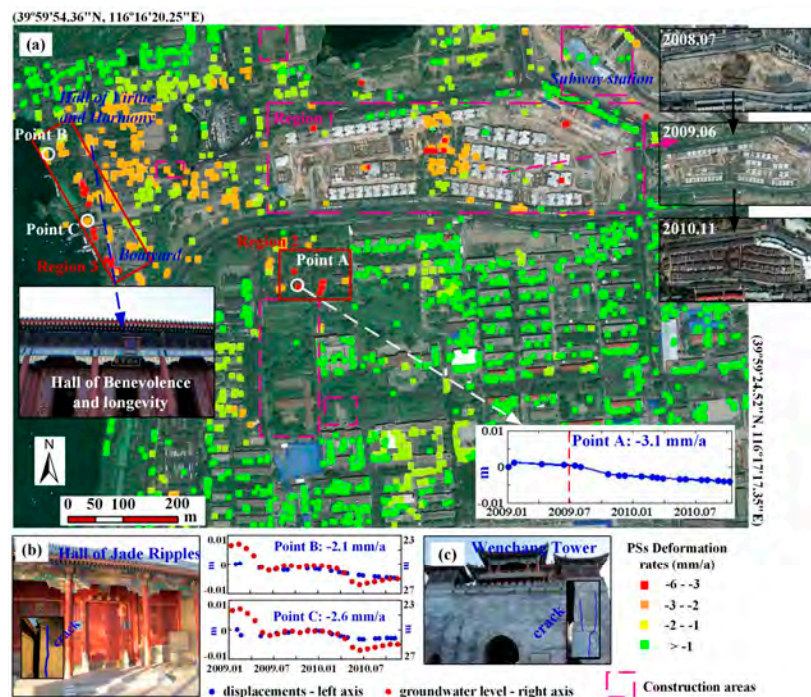


**Figure 7.** (a) Map of deformation rates in the East Gate region superimposed on the Google Earth image acquired in June 2009. Constructions during 2009–2010 and their impacted neighborhoods are marked as pink and red dashed-boxes; (b,c) Photographs of Points B and C, respectively. The graphs illustrate the displacement evolution (blue dots) of Points A–C. The red dashed line in the evolution of Point A was used to mark the starting time of the construction activity in the south. Groundwater data (red dots) were used to validate the displacement evolution of Points B and C.

Figure 7 illustrates the regional subsidence of MTInSAR results. Region 1 refers to a stretch of residential quarters built in the period from 2008 to 2011. The drastic surface changes here resulted in the absence of PSs except for the location of the central subzone where construction was completed before the acquisitions of SAR images. PSs in this region exhibited a significant subsidence trend with deformation rates ranging from  $-2.0$  to  $-4.0$  mm/a. In Region 2, a group of bungalow-type accommodations were identified as PSs. Instabilities were detected, such as in Point A with a deformation rate of  $-3.1$  mm/a. A subsidence event occurred in the period from June to September 2009, immediately after the construction in the south, placing the responsibility on construction behavior for instabilities in Region 2. Thorough maintenance work was launched since 2014 for the conservation of relics. All historic remains around the East Gate of the Summer Palace, including the Hall of Virtue and Harmony, Hall of Benevolence and Longevity and Wenchang Yard, indicate a moderate subsidence with LOS deformation rates ranging from  $-3.0$  to  $-2.0$  mm/a. Renovation and/or consolidation countermeasures are urgently needed. Motion sensors have been installed by administrators for the monitoring of destructive motions. Measurements of them confirmed the instability phenomenon in this area.

Significant subsidence was mainly detected on the artifacts (including halls, shopping centers, a boatyard and tower) along the Kunming Lakeside of Region 3. Point B refers to the Hall of Jade Ripples (see Figure 7b). It used to be the emperor's living quarters (the emperor of Guangxu was once imprisoned here). The corresponding deformations, with a rate of  $-2.1$  mm/a, were modulated by the fluctuation associated with the seasonal variation of the water-level of Kunming Lake. A long crack on the wall was observed during field investigations. Deformation rates of over  $-3.0$  mm/a were detected on shopping facilities, demonstrated by consecutive PSs in Region 3. Point C is located on the two-story Wenchang Tower (see Figure 7c). Wall cracks are clearly visible although they have been whitewashed several times. Evolution of Points B and C indicates a consistent trend compared with

the variations of groundwater level, implying the impact of hydrological disturbances. Additionally, excessive and unsustainable tourism together with the lack of maintenance could also contribute to the defects observed.

### (3) Kunming Lakeside and Islands

In addition to Longevity Hill and East Gate, Kunming Lake and its islands are also historic and cultural components of the Summer Palace. MTInSAR-derived deformations show relics in the islands were subsiding (Figure 8). Region 1 refers to an area close to the South Lake Island. A piece of land was under construction that exerted a negative impact for the stability of relics inside the site (see Figure 8b). The Spacious Pavilion, located at the starting point of the Seventeen Arches Bridge (connecting the mainland and the South Lake Island), is the biggest historic pavilion-style building in China (more than 130 square meters). PSs-derived motions attested to the stability of this building. In contrast, at the boatyard named Bafang LOS deformation rates of approximately  $-3.6$  mm/a (Point A) were detected. The South Lake Island, covering an area of over one hectare, is situated in the southeast part of Kunming Lake. Emperors and empresses used to enjoy the scenery and watch the navy performances here. Historic buildings, including the Temple of Dragon King, Hall of Distant View, Hall of Moon and Wave and Hall of Cloud and Incense, were all burned down in 1860 and rebuilt on this island. PSs-derived motions indicate that the whole island is subsiding with an average deformation rate of  $-2.0$  mm/a (Point B). Both Points A and B exhibited a seasonal motion fluctuation associated with the water-level variation of the lake.

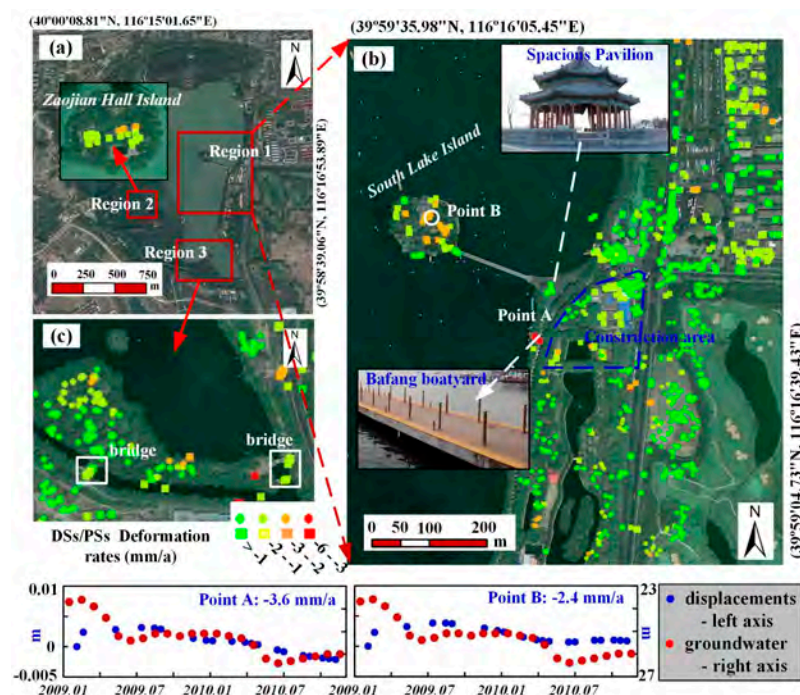


**Figure 8.** (a) Google Earth map of the study site and the deformation map of Zaojian Hall Island; (b) map of deformation rates in Region 1 and the displacement time series of Points A and B; and (c) map of deformation rates in Region 3. The graphs illustrate displacement evolution of Points A and B (blue dots) together with the change of groundwater level (red dots).

Sinking was also observed in the island of Zaojian Hall (used to be the place for reading, writing and painting), as illustrated by the Region 2 in Figure 8a and is attributable to the decline of groundwater level during 2009–2010 (see Figure 2b). In the vicinity of the South Gate (Region 3), plenty of DSs (open area with trees) and PSs (man-made structures) were extracted; unstable trends with the maximum rate of  $-3.3$  mm/a, particularly for features associated with the bridges (Figure 8c), were observed.

#### (4) Surrounding Landscapes

The surrounding landscape of the Summer Palace had experienced significant changes since 2009. Intense human activities within red-rectangles (see Figure 9a) threatened the safeguarding of precious heritage features. In this section, three representative regions were selected for deformation analysis. Region 1 refers to the residential district where at least three sub-zones were under construction or demolition (see Figure 9b) in 2009, initiating instabilities among neighborhood buildings; e.g., Point A with the rate of  $-3.6$  mm/a. Region 2 shows a sparsely vegetated area with several houses nearby the lakeside (see Figure 9c). This area used to be a farmland but has been redeveloped as a park. A regional surface subsidence was detected by DSs ( $-2.0$ ~ $-1.0$  mm/a) due to the construction of a road. Region 3 experienced significant changes (see Figure 9d). First, a village named Liulang was almost completely demolished due to urbanization except for a primary school at the southeast of Kunming Lake. PSs were identified on the houses before the demolition (started in 2011, immediately after the completion of SAR data acquisitions). Deformation results during 2009–2010 indicate that this residential site was unstable particularly along the peripheries (with the maximum subsidence of  $-3.0$  mm/a) due to preparations for demolitions. Second, a highway and a factory were built in 2008 and 2009, respectively, in the south side of the South Gate. Deformation results indicate that the highway was subsiding, with a maximum rate of over  $-4.0$  mm/a. In contrast, a steady condition was observed along the roadside using the DSs-derived deformations. Third, as one component of the “Water Diversion Project”, a riverway was constructed during 2006–2009. All buildings surrounding Point A had been demolished before 2012 (see the historic Google Earth images in Figure 9d). Point A, with a LOS deformation rate of  $-3.1$  mm/a, indicated the instabilities of this region caused by the construction and demolition activities.

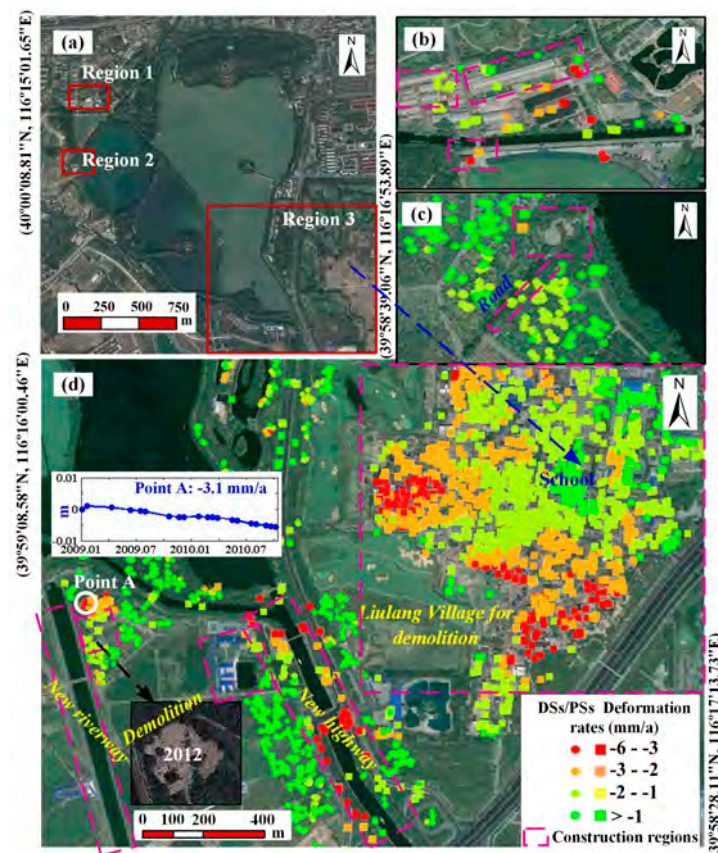


**Figure 9.** (a) Google Earth map of the subzone; (b) map of deformation rates in Region 1; (c) map of deformation rates in Region 2; and (d) map of deformation rates in Region 3. Displacement time series of Points A and B are also shown. Regions under construction are marked by pink dashed boxes.

## 5.2. Summary of Validations

In this study, several solutions have been proposed for the validation of the MTInSAR-derived results. They can be summarized as follows: First, Google Earth images were applied for identifying deformation as well as construction events that are closely linked to the subsidence triggering. Second, groundwater data from boreholes in downtown of Beijing City were collected to analyze the relationship between local hydrology and structural instabilities observed along the Kunming Lake, indicating a consistent decline trend in 2009–2010. Third, several field investigations were undertaken to assess the status of monuments; for instance, cracks were observed in points where the occurrence of significant motions were detected from SAR data. Electrical sensors, installed in the Hall of Virtue and Harmony by local administrators, showed that the historic structures in this area were unstable, which was also detected by the MTInSAR-derived results with deformation rates in the range of  $-3.0\sim-2.0$  mm/a.

## 6. Conclusions

In this study, an advanced MTInSAR approach for monitoring deformation risks of cultural heritage sites surrounded by a semi-natural landscape was tested using high-resolution space-borne SAR images. Compared to ground-based surveying (e.g., leveling, GPS and geophysical prospecting), MT-InSAR approaches have significant advantages: first, MTInSAR techniques perform better in detecting subtle deformations due to the high-precision (up to mm level), low-cost and non-intrusive tools used. Second, thanks to the high resolution and broad coverage of SAR images, a two-scale surveillance scheme from a single monument to the entire heritage site is feasible; this allows a systematic diagnosis of the entire site as well as its surrounding landscape through instability measurements based on PSs/DSs. Third, the advanced MTInSAR approach proposed in this study is more powerful in dealing with the semi-natural landscape surrounding the cultural heritage site by integrating PSs and DSs as well as the small baseline strategy applied.

The Summer Palace was chosen as the experimental site to present the potential of the proposed MTInSAR methodology. Stability was characteristic of most monuments but there were a few regions of instability and deformation. Main conclusions drawn from the results include the following:

- (1) The introduction of DSs improves the monitoring capability of the MT-InSAR approach. Several ruins (such as Gaichun Yuan, WeixianZhai and Qiwang Xuan) on Longevity Hill, partly overshadowed by woods, were successfully identified and monitored by extracted DSs.
- (2) From 2009 to 2011, enormous changes to the landscape were accompanied by land subsidence in the vicinity of the Summer Palace, resulting in region-wide instabilities of historic remains especially in areas adjacent to East and South Gates. Urbanization including construction and demolition activities associated with buildings and roads were the primary triggers for the deformation observed.
- (3) On Longevity Hill, monuments were generally stable except for some of the ruins, monuments and areas near shops and boatyards. The ruins, such as Gaichun Yuan, WeixianZhai and Qiwang Xuan, suffered from mm/cm-level subsidence, which was interpreted to be resulting from a mix of impacts from human activities and natural decay. Archaeological excavations in Sidabuzhou may also have contributed to triggering instabilities around that site.
- (4) Subsidence trends in historic buildings, shops and boatyards along the Kunming Lakeside or in the islands showed the seasonal fluctuations associated with the variation of the groundwater level. Excessive tourism and the lack of maintenances also contributed to the instability phenomena observed along the Lakeside.

**Acknowledgments:** This work was supported by funding from Hundred Talents Program of the Chinese Academy of Sciences (CAS) (Y5YR0300QM) and Youth Director Fund Category-A of Institute of Remote Sensing and Digital Earth, CAS.

**Author Contributions:** Panpan Tang wrote the program of methodology and interpreted the MTInSAR-derived results together with Fulong Chen. Xiaokun Zhu collected the SAR data and did the basic SAR data processing.

Wei Zhou contributed to field investigations and thematic data processing. Panpan Tang and Fulong Chen drafted the manuscript. All authors contributed to the finalization of this paper.

**Conflicts of Interest:** The authors declare no conflict of interest.

## References

1. Guo, H.D. Front matter. In *Atlas of Remote Sensing for World Heritage: China*; Springer Berlin Heidelberg: Heidelberg, Germany, 2013; pp. VII–XI.
2. Glisic, B.; Inaudi, D.; Posenato, D.; Figini, A.; Casanova, N. Monitoring of heritage structures and historical monuments using long-gage fiber optic interferometric sensors—An overview. In Proceedings of the 3rd International Conference on Structural Health Monitoring of Intelligent Infrastructure-SHMII-3, Vancouver, BC, Canada, 13–16 November 2007.
3. Zhou, W.; Chen, F.L.; Guo, H.D. Differential radar interferometry for structural and ground deformation monitoring: A new tool for the conservation and sustainability of cultural heritage sites. *Sustainability* **2015**, *7*, 1712–1729. [[CrossRef](#)]
4. Katz, O.; Crouvi, O. The geotechnical effects of long human habitation (2000<years): Earthquake induced landslide hazard in the city of Zefat, Northern Israel. *Eng. Geol.* **2007**, *95*, 57–78.
5. Gigli, G.; Frodella, W.; Mugnai, F.; Tapete, D.; Cigna, F.; Fanti, R.; Intrieri, E.; Lombardi, L. Instability mechanisms affecting cultural heritage sites in the Maltese Archipelago. *Nat. Hazards Earth Syst. Sci.* **2012**, *12*, 1883–1903. [[CrossRef](#)]
6. Ferretti, A.; Prati, C.; Rocca, F. Permanent scatterers in SAR interferometry. *IEEE Trans. Geosci. Remote Sens.* **2001**, *39*, 8–20. [[CrossRef](#)]
7. Berardino, P.; Fornaro, G.; Lanari, R.; Sansosti, E. A new algorithm for surface deformation monitoring based on small baseline differential SAR interferograms. *IEEE Trans. Geosci. Remote Sens.* **2002**, *40*, 2375–2383. [[CrossRef](#)]
8. Ferretti, A.; Fumagalli, A.; Novali, F.; Prati, C.; Rocca, F.; Rucci, A. A new algorithm for processing interferometric data-stacks: SqueeSAR. *IEEE Trans. Geosci. Remote Sens.* **2011**, *49*, 3460–3470. [[CrossRef](#)]
9. Tapete, D.; Cigna, F. Site-specific analysis of deformation patterns on archaeological heritage by satellite radar interferometry. In *MRS Proceedings*; Cambridge University Press: Cambridge, UK, 2012; Volume 1374, pp. 283–295.
10. Tapete, D.; Fanti, R.; Cecchi, R.; Petrangeli, P.; Casagli, N. Satellite radar interferometry for monitoring and early-stage warning of structural instability in archaeological sites. *J. Geophys. Eng.* **2012**, *9*, S10–S25. [[CrossRef](#)]
11. Tapete, D.; Cigna, F. Rapid mapping and deformation analysis over cultural heritage and rural sites based on persistent scatterer interferometry. *Int. J. Geophys.* **2012**. [[CrossRef](#)]
12. Tapete, D.; Morelli, S.; Fanti, R.; Casagli, N. Localising deformation along the elevation of linear structures: An experiment with space-borne InSAR and RTK GPS on the Roman Aqueducts in Rome, Italy. *Appl. Geogr.* **2015**, *58*, 65–83. [[CrossRef](#)]
13. Fomelis, M.; Pavlopoulos, K.; Kourkoulis, P. Ground deformation monitoring in cultural heritage areas by time series SAR interferometry: The case of ancient Olympia site (Western Greece). In Proceedings of the ESA FRINGE Workshop, Frascati, Italy, 30 November–4 December 2009.
14. Zeni, G.; Bonano, M.; Casu, F.; Manunta, M.; Manzo, M.; Marsella, M.; Pepe, A.; Lanari, R. Long-term deformation analysis of historical buildings through the advanced SBAS-DInSAR technique: The case study of the city of Rome, Italy. *J. Geophys. Eng.* **2011**, *8*, S1–S12. [[CrossRef](#)]
15. Goel, K.; Adam, N. An advanced algorithm for deformation estimation in non-urban areas. *ISPRS J. Photogramm.* **2012**, *73*, 100–110. [[CrossRef](#)]
16. Tang, P.P.; Chen, F.L.; Guo, H.D.; Tian, B.S.; Wang, X.Y.; Ishwaran, N. Large-area landslides monitoring using advanced multi-temporal InSAR technique over the giant panda habitat, Sichuan, China. *Remote Sens.* **2015**, *7*, 8925–8949. [[CrossRef](#)]
17. Wegmüller, U.; Werner, C. Gamma SAR Processor and Interferometry Software. Available online: <http://earth.esa.int/workshops/ers97/papers/wegmuller2/> (accessed on 8 July 2015).

18. Cigna, F.; Lasaponara, R.; Masini, N.; Milillo, P.; Tapete, D. Persistent scatterer interferometry processing of COSMO-SkyMed Stripmap Himage time series to depict deformation of the historic centre of Rome, Italy. *Remote Sens.* **2014**, *6*, 12593–12618. [[CrossRef](#)]
19. Monti Guarnieri, A.; Tebaldini, S. A new framework for multi-pass SAR interferometry with distributed targets. In Proceedings of the IEEE International Geoscience and Remote Sensing Symposium, Barcelona, Spain, 23–28 July 2007; pp. 5289–5293.
20. Deledalle, C.A.; Denis, L.; Tupin, F.; Reigber, A.; Jager, M. NL-SAR: A unified nonlocal framework for resolution-preserving (Pol) (In) SAR Denoising. *IEEE Trans. Geosci. Remote Sens.* **2015**, *53*, 2021–2037. [[CrossRef](#)]
21. Vasile, G.; Trouvé, E.; Lee, J.S.; Buzuloiu, V. Intensity-driven adaptive-neighborhood technique for polarimetric and interferometric SAR parameters estimation. *IEEE Trans. Geosci. Remote Sens.* **2006**, *44*, 1609–1621. [[CrossRef](#)]
22. Byrd, R.H.; Lu, P.; Nocedal, J.; Zhu, C.A. Limited memory algorithm for bound constrained optimization. *SIAM J. Sci. Stat. Comput.* **1995**, *16*, 1190–1208. [[CrossRef](#)]
23. Pepe, A.; Lanari, R. On the extension of the minimum cost flow algorithm for phase unwrapping of multi-temporal differential SAR interferograms. *IEEE Trans. Geosci. Remote Sens.* **2006**, *44*, 2374–2383. [[CrossRef](#)]



© 2016 by the authors; licensee MDPI, Basel, Switzerland. This article is an open access article distributed under the terms and conditions of the Creative Commons Attribution (CC-BY) license (<http://creativecommons.org/licenses/by/4.0/>).